NASA Technical Memorandum 106256

Stress-Rupture Behavior of Small Diameter Polycrystalline Alumina Fibers

Hee Mann Yun
Cleveland State University
Cleveland, Ohio

Jon C. Goldsby
Lewis Research Center
Cleveland, Ohio

and

James A. DiCarlo
Lewis Research Center
Cleveland, Ohio

Prepared for the
95th Annual Meeting and Exposition of the American Ceramic Society
Cincinnati, Ohio, April 18–23, 1993

NASA

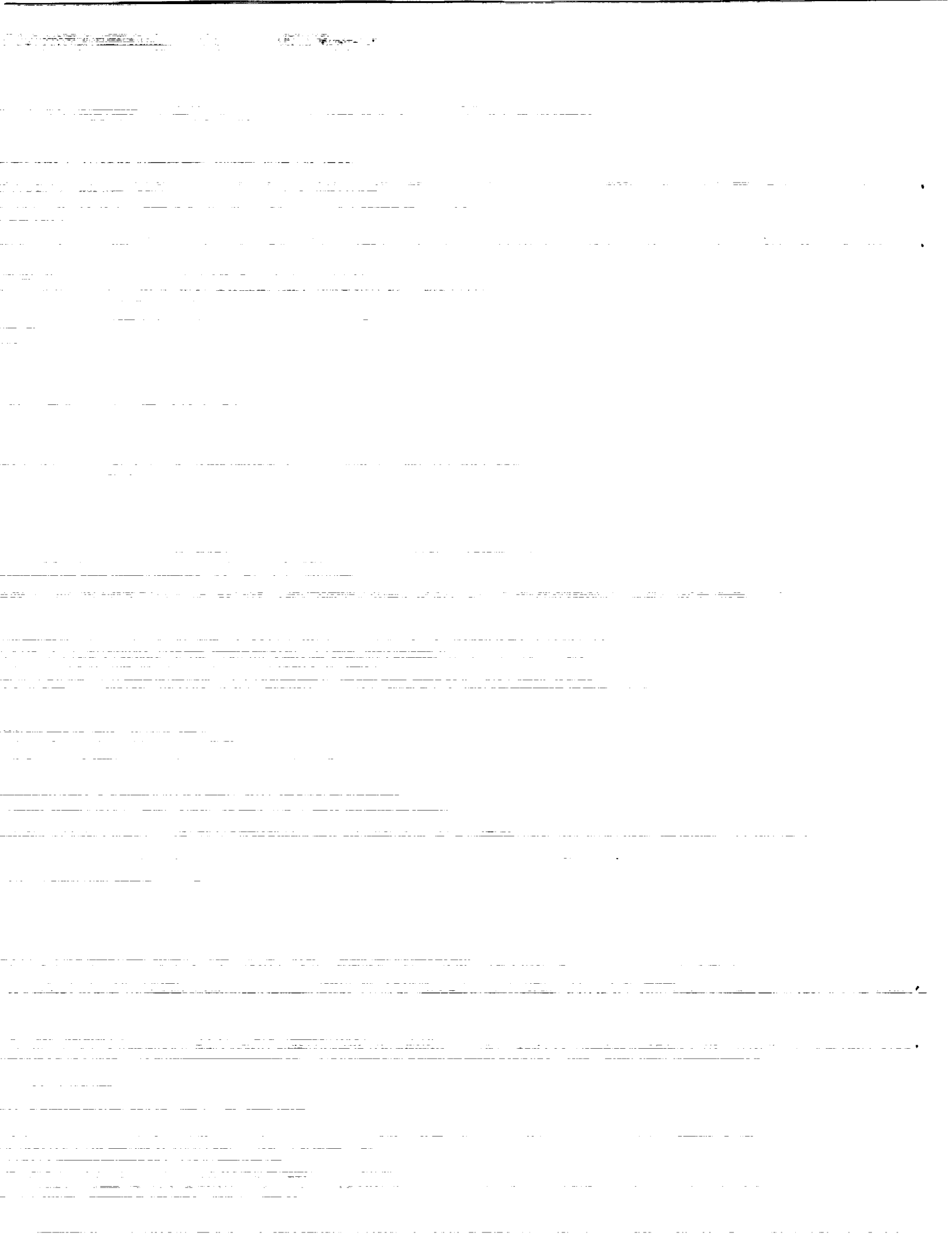

STRESS-RUPTURE BEHAVIOR OF SMALL DIAMETER POLYCRYSTALLINE ALUMINA FIBERS

H.M. Yun,* J.C. Goldsby, and J.A. DiCarlo
National Aeronautics and Space Administration
Lewis Research Center
Cleveland, Ohio 44135

Abstract

Continuous length polycrystalline alumina fibers are candidates as reinforcement in high temperature composite materials. Interest therefore exists in characterizing the thermomechanical behavior of these materials, obtaining possible insights into underlying mechanisms, and understanding fiber performance under long term use. In this paper, results are reported on the time-temperature dependent strength behavior of Nextel 610 and Fiber FP alumina fibers with grain sizes of 100 and 300 nm, respectively. Below 1000 °C and 100 hr, Nextel 610 with the smaller grain size had a greater fast fracture and rupture strength than Fiber FP. The time exponents for stress-rupture of these fibers were found to decrease from ~13 at 900 °C to below 3 near 1050 °C, suggesting a transition from slow crack growth to creep rupture as the controlling fracture mechanism. For both fiber types, an effective activation energy of 690 kJ/mol was measured for rupture. This allowed stress-rupture predictions to be made for extended times at use temperatures below 1000 °C.

---

*Resident Research Associate from Cleveland State University, Cleveland, Ohio 44115.

INTRODUCTION

Continuous length polycrystalline alumina fibers offer excellent potential as reinforcement for composite materials [1]. Among their benefits are their commercial availability, chemical stability, and thermostability in most environments, as well as their small diameter which makes them capable of being woven into two- and three-dimensional architectures. Because of this potential, there is current interest in evaluating the thermomechanical behavior of these fibers in order to select those types which will satisfy the design requirements of various metal and ceramic high temperature composites. In this regard, a number of key properties must be evaluated. For example, creep strain as a function of time, temperature, and applied stress must be known to understand what conditions will allow the composite to remain within strict dimensional tolerances required by the application [2]. One must also know the strength stability of these reinforcements under benign, nonstructural conditions in order to have insight into their abilities to withstand random overloads [3]. Fracture studies under dynamic and continuous loading conditions are also needed to determine the stress, temperature, and lifetime limits for structural applications. These types of studies can also provide insights as to the mechanisms involved in the deformation and fracture processes which may help guide fiber development and improvement.

The primary objective of this study was to generate high temperature dynamic strength and stress-rupture data for two polycrystalline alumina fibers: Nextel 610 and Fiber FP fabricated by 3M Company [4] and E.I. du Pont de Nemours & Company, respectively. Since these fibers have measurably different grain sizes and impurity phases, significant differences in high temperature strength were expected. A second objective was to perform an analysis of the data in order to identify the underlying microstructural mechanisms and to project long time rupture behavior at high temperature.

EXPERIMENTAL

As indicated in Table 1, the compositions of the fibers used in this study was more than 99 percent alumina with additions of SiO_2 and Fe_2O_3 for Nextel 610 and MgO for Fiber FP. These additives serve as aids to consolidation and as microstructural control agents (in particular against grain growth). The diameters of these fibers were nominally 14 and 20 μm for the Nextel 610 and Fiber FP with average grain size of 100 and 300 nm [2], respectively.

Table 1.—Nominal Properties of Polycrystalline Alumina Fibers

Property \ Fiber	Nextel 610	Fiber FP
Manufacturer	3M	DuPont
Composition, wt %	>99 α-Al_2O_3	>99 α-Al_2O_3
Impurities, wt %	0.2-0.3 SiO_2	~0.3 MgO
	0.4-0.7 Fe_2O_3	
Average diameter, μm	14	20
Elastic modulus at RT, GPa	~380	~380
Average grain size, μm	0.1	0.3

For this investigation, stress-rupture measurements were made by dead weight loading. Dynamic tensile strength measurements were also made as a function of stress rate in a commercial load frame. The test temperatures were in the range from 800 to 1100 °C with loading times from 1 min to 100 hr. The tests were done mostly in air, but some experiments were done in a vacuum of 10^{-5} Pa with no observable difference in the results.

In performing the stress-rupture tests, hot grips were used for dead weight loading at low stress (Fig. 1). These grips were constructed by using a

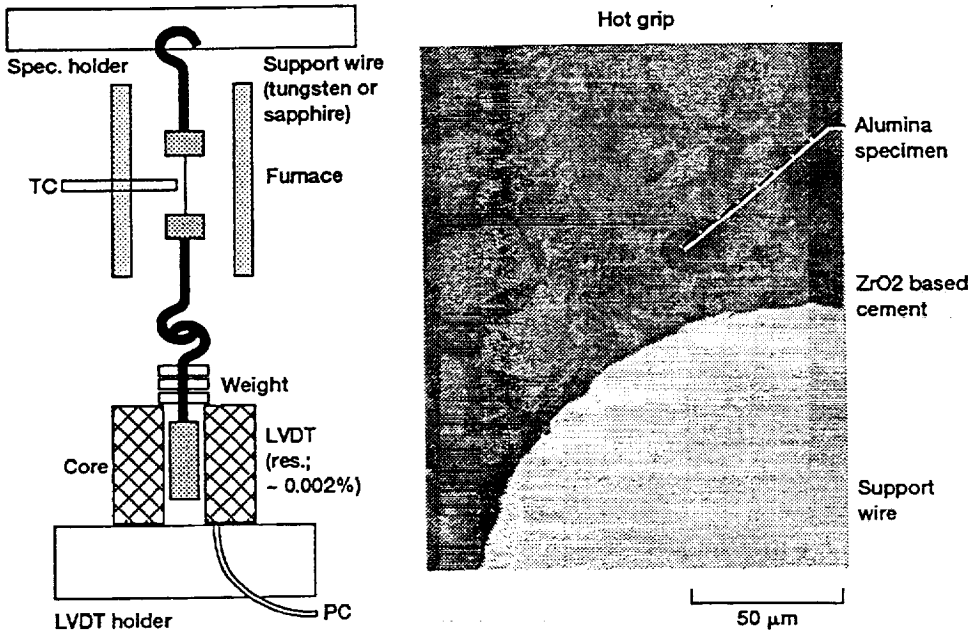

Figure 1.—Single filament creep and stress-rupture rig (gauge length of 25 mm).

125-μm diameter sapphire fiber as top and bottom support wires and securing the fiber specimen with a high temperature zirconia base cement (manufactured by the Sauereisen Cements Company of Pittsburgh, Pennsylvania). This cement did not interact with the specimen nor did it allow slippage at the temperatures and stress levels used in this investigation. Small diameter (125 μm) tungsten wire hooks were used to minimize bending moments in the load train. The specimen's gage length was nominally 25 mm.

For the rupture tests at high stress, cold grips were used with grip-to-grip fiber lengths of 180 mm. A hot zone length of ~25 mm was provided by the test furnace which contained molydisilicide heating elements and was capable of continuous operation in air up to 1500 °C. A Pt-Rh thermocouple and electronic controller provided a constant temperature hot zone within ±2 °C. The maximum thermal gradient along the hot zone was 0.25 °C/mm. The same furnace and a cold grip setup was used for the high temperature stress rate tests.

The fiber diameters used in the strength determinations were obtained from the average of 40 specimens as measured at room temperature with a split image microscope and verified with SEM cross-sectional micrographs. These values were 14.6 (±2.2) μm for the Nextel 610 and 18.7 (±2.6) μm for the Fiber FP.

RESULTS

Figure 2 displays the effects of stress rate on the fast fracture tensile strength of Nextel 610 at 980 °C. These results are presented in the form of a Weibull plot [5,6]. The stress rates used were 0.8 to 40 MPa/sec and the duration of the test was 1 to 40 min. Key points to notice from these data are that, by increasing the stress rate by a factor of 50, the average tensile strength increased by 2, and that the Weibull modulus was not affected by stress rate, suggesting no change in the flaw population. In this case, an average Weibull modulus value of 5.5 was obtained.

The stress-rupture strength was also measured for Nextel 610 and Fiber FP under constant load and the results are illustrated in Figs. 3(a) and (b), respectively. Again a time dependence was observed in the stresses necessary to obtain rupture or fracture. However, a significant difference in the behavior of the two fiber types was observed. For example, at 900 °C for rupture times from 6 min to 100 hr, stresses from 1500 to 700 MPa were needed

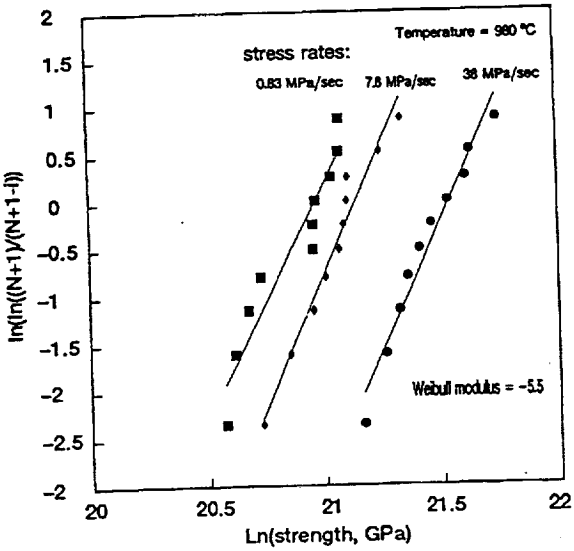

Figure 2.—Stress rate effects on failure probability of Nextel 610.

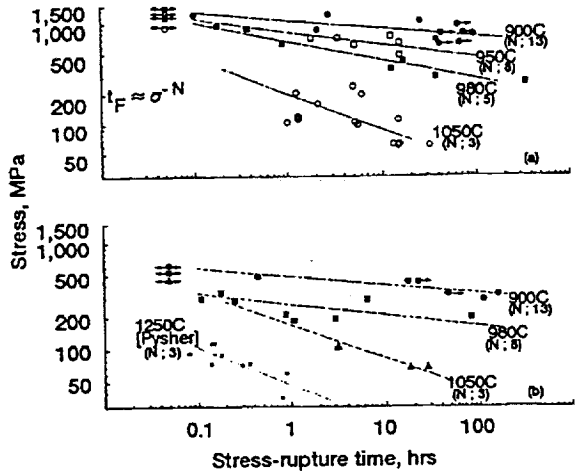

Figure 3.—Stress-rupture strength of (a) Nextel 610 and (b) Fiber FP.

for the Nextel 610, whereas stresses from 600 to 350 MPa were needed for rupture of Fiber FP.

Figure 3 also shows that stress-rupture life was more sensitive to stress at higher temperatures than at lower temperatures for both fibers. The stress-rupture time exponent, N, was obtained from the slope of the best fit lines

on a log-log plot of stress versus rupture time. That is, it was assumed that rupture strength, σ_{sr}, was related to the fracture time, t_f, by the equation

$$\sigma_{sr} = \left(t_f\right)^{-1/N} \tag{1}$$

For both fibers the N exponent at 900 °C was ~13 and decreased to about 3 at 1050 °C. The low exponent is similar to the value obtained from Pysher [7] at 1250 °C for the Fiber FP in which creep rupture was found to be the mode of failure.

DISCUSSION

There appears to be two different fracture mechanisms operating in the polycrystalline alumina fibers of this study. One mechanism is slow crack growth (SCG) in which pre-existing cracks grow to a critical size which then causes rupture to occur. The second mechanism involves the nucleation and coalescence of creep generated cavities to form the critical flaw [8,9]. Stress-rupture from SCG of pre-existent flaws has characteristically higher time exponents, N, than creep rupture (CR) in which case the Monkman-Grant relation predicts time exponents, approximately equal to the stress exponents in power law creep. In a previous study [3], these stress exponents in the steady-state creep regime were determined to be about 3 and 1 for the Nextel 610 and Fiber FP, respectively. Thus for those stress-time-temperature conditions in which $N > 3$, it is assumed that the rupture mechanism is related to slow crack growth, whereas for those conditions in which $N < 3$, creep rupture by cavitation is probably controlling.

In the case of SCG, linear fracture mechanics allow relationships between crack propagation and rupture times to be calculated [10,11,12]. For example, if SCG in the fibers is the cause of fracture, then the rupture time exponent N can also be indirectly obtained from the dynamic stress rate tests. A crack propagation time exponent of $N = 5$ was measured from dynamic fast fracture tests at 980 °C (Fig. 2). This value was determined from the slope of the best fit line of a log-log plot of stress rate $d\sigma/dt$ versus the average failure stress σ through the relation,

$$N = \frac{\Delta \log\left(\frac{d\sigma}{dt}\right)}{\Delta \log(\sigma)} - 1 \qquad (2)$$

The N = 5 value is in agreement with the time exponent obtained from the static stress-rupture tests performed at short times at the same temperature (cf. Fig. 3). This is indicative of a SCG mechanism being operative, which may be causing stress-rupture in Nextel 610 at 980 °C. In addition, the relatively high values obtained for time exponent between 900 and 980 °C for Nextel 610 gives further support for the SCG mechanism. Therefore we deduce that the drop in the stress-rupture strength of Nextel 610 is caused by SCG. In contrast Fiber FP exhibits a higher rupture strength, but above 1050 °C, the strength degrades in what is considered an effectively creep-rupture region as defined by its stress and temperature range (as identified by Pysher [7]).

Stress-rupture when controlled by a thermally activated process can be described by various empirical parameters such as the well-known Larson-Miller [13], Dorn [14], or Manson-Haferd [15] parameters. These parameters include such factors as temperature, rupture time, and other constants depending upon which parameters warrant attention. The experimental evidence obtained in this study strongly infers that the high temperature fracture processes of the alumina fibers are also governed by thermally activated mechanisms. We therefore propose that the stress required for rupture, σ_{sr}, can be expressed as a function of a thermal activation parameter θ; that is

$$\sigma_{sr} = F(\theta) \qquad (3)$$

where

$$\theta = t_f \exp\left(\frac{-Q_{sr}}{RT}\right). \qquad (4)$$

Here Q_{sr} is the effective activation energy for stress-rupture, R is the universal gas constant, and T the absolute temperature.

For constant σ_{sr}, θ will be constant so that

$$Q_{sr} = R \frac{\Delta \ln\left(t_f\right)}{\Delta\left(\frac{1}{T}\right)} . \tag{5}$$

With these relationships, stress-rupture data at different times and temperatures can be used to determine Q_{sr} for the two fibers. For example, for a given σ_{sr} value, Q_{sr} can be obtained by Eq. (5) from the slope of a semi-logarithmic plot of the rupture time versus the reciprocal temperature. Figure 4 shows such a plot for the Nextel 610 and Fiber FP from which a

Q_{sr} of 690 kJ/mol was determined for both fiber types. The activation energy is apparently independent of stress level suggesting that it applies both to SCG and creep rupture mechanisms. That is to say, mechanisms responsible for the coalescence or linking-up of subcritical, size flaws into critical flaws are the same for SCG and creep rupture. The difference between these modes of failure is in the creation of the subcritical flaws. In the case of SCG, pre-existing microstructural features initiate noncritical cracks and within the stress field ahead of the crack tip, microvoids form. It is these voids that coalesce into the critical flaws. In creep rupture however, the creation of cavities at the grain boundaries form subcritical sized flaws that coalesce to failure [17,18].

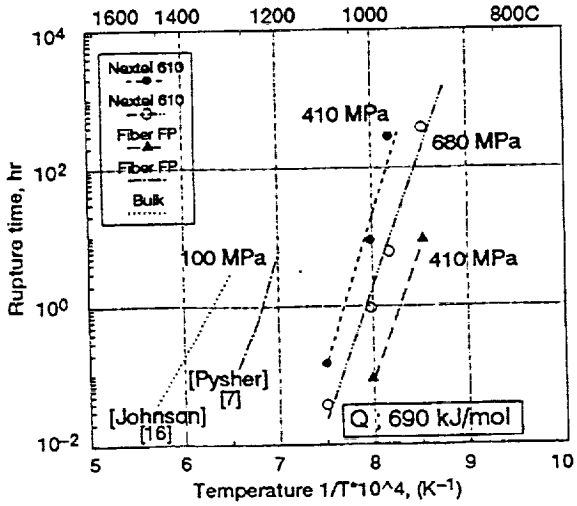

Figure 4.—Activation energy for stress-rupture behavior of Polycrystalline Alumina fibers

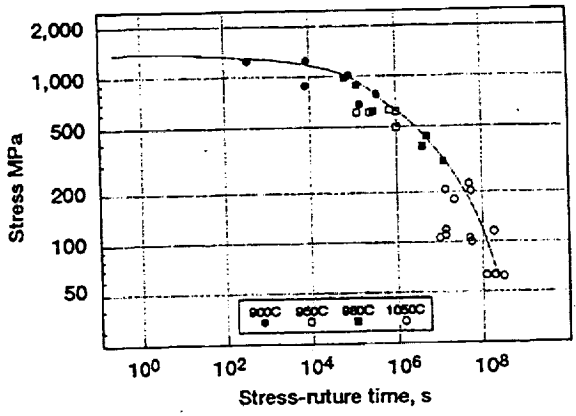

Figure 5.—Master curve for stress-rupture strength of Nextel 610 fiber at 900 °C.

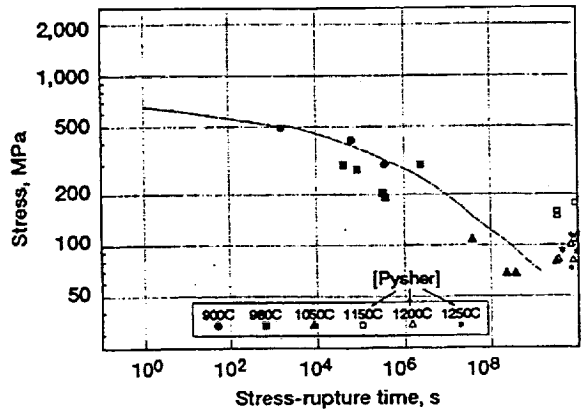

Figure 6.—Master curve for stress-rupture strength of FP Alumina fiber at 900 °C.

In order to project rupture behavior for long times, Eqs. (3) and (4) can now be used to generate a master stress-rupture curve at any temperature T_0 and time t_0 by the relation:

$$\ln\left(\frac{t_0}{t_f}\right) = \frac{Q_{sr}}{R}\left(\frac{1}{T_0} - \frac{1}{T}\right) \tag{6}$$

where t_f and T are the rupture time and temperature in which a certain rupture strength was measured. Using Eq. (6), master rupture curves were generated at 900 °C for Nextel 610 and Fiber FP as illustrated in Figs. 5 and 6, respectively. On the basis of the data obtained in this study (note keys in Figs. 5 and 6), projections of rupture strength of up to 3 years at 900 °C are

predicted. As an example, of how this curve could be practically used, consider a composite system requiring a 500-MPa fiber rupture strength at 900 °C. Nextel 610 would meet this requirement for about 300 hr whereas Fiber FP would meet this requirement for only 3 hr.

CONCLUSIONS

Nextel 610 and Fiber FP polycrystalline alumina fibers show significant differences in stress-rupture behavior that are probably related to grain size and grain boundary phases. In general, due most likely to its smaller grain size, Nextel 610 has better strength properties at short times and low temperature; whereas Fiber FP performs better at long time and higher temperatures (above 1000 °C). For Fiber FP, this higher temperature capability can only be attained at very low stresses and thus this fiber is not suitable for load bearing structural composites. On the basic side, experimental evidence strongly suggests that the predominating mechanisms controlling degradation of fiber strength at elevated temperature are slow crack growth in Nextel 610 and creep rupture (cavitation) in Fiber FP.

REFERENCES

[1] M.H. Stacy, "Development in Continuous Alumina-Based Fibers," Br. Ceram. Trans. J., **87**, 168–172 (1988).

[2] H.M. Yun and J.C. Goldsby, "Tensile Creep Behavior of Polycrystalline Alumina Fibers," Presented at the 17th Annual Conference and Exposition on Composites and Advanced Ceramics (Restricted Sessions) Cocoa Beach, FL, Jan. 11–14, 1993.

[3] J.C. Goldsby, "Thermomechanical and Microstructural Stability of Polycrystalline Alumina Fiber," Presented at the 17th Annual Conference and Exposition on Composites and Advanced Ceramics (Restricted Sessions), Cocoa Beach, FL, Jan. 11–14, 1993.

[4] M.M. Vogel-Martin and D.M. Wilson, "Properties of Seeded Sol-Gel Alumina Fiber," pp. 519–522 in The Sixteenth Conference on Metal Matrix, Carbon, and Ceramic Matrix Composites, NASA CP–3175, Pt. 2, 1992.

[5] S.N. Patankar, "Weibull Distribution as Applied to Ceramic Fibers," J. Mater. Sci. Let., **10**, 1176–1181 (1991).

[6] K.K. Smyth and M.B. Magida, "Dynamic Fatigue of a Machinable Glass-Ceramic," J. Am. Ceram. Soc., **66** [7] 500–505 (1983).

[7] D.J. Pysher and R.E. Tressler, "Tensile Creep Rupture Behavior of Alumina-Based Polycrystalline Oxide Fibers," Ceram. Eng. Sci. Proc., **13** [7–8] 218–226 (1992).

[8] F.C. Monkman and N.J. Grant, "An Analytical Relationship Between Rupture Life and Minimum Creep Rate in Creep-Rupture Tests," Proc. ASTM, **56**, 593 (1956).

[9] D.C. Cranmer, B.J. Hockey, and S.M. Wiederhorn, "Creep and Creep Rupture of HIP'ed Si3N4," Ceram. Eng. Sci. Proc., **12** [9–10] 1862–1872 (1991).

[10] J.E. Ritter, Jr., "Engineering Design and Fatigue Failure of Brittle Materials," in Fracture Mechanics of Ceramics, Crack Growth and Microstructure, pp. 667–686. Edited by R.G. Bradt, D.P.H. Hasselman, and F.F. Lange. Plenum Press, New York, 1978.

[11] K. Jakus, D.C. Coyne, and J.E. Ritter, Jr., "Analysis of Fatigue Data for Lifetime Predictions for Ceramic Materials," J. Mater. Sci., **13**, 2071–2080 (1978).

[12] A.G. Evans, "Slow Crack Growth in Brittle Materials under Dynamic Loading Conditions," Intern. J. Frac., **10** [2] 251–259 (1974).

[13] F.R. Larson and J. Miller, "Time-Temperature Relationship for Rupture and Creep Stresses," Trans. ASME, **74**, 765–774 (1952).

[14] R.L. Orr, O.D. Sherby, and J.E. Dorn, "Correlations of Rupture Data for Metals at Elevated Temperatures," Trans. ASM, **46**, 113–156 (1954).

[15] S.S. Manson and A.M. Haferd, "A Linear Time-Temperature Relation for Extrapolation of Creep and Stress-Rupture Data," NACA TN–2890, Mar. 1953.

[16] S.M. Johnson, B.J. Dalgleish, and A.G. Evans, "High Temperature Failure of Polycrystalline Alumina," J. Am. Ceram. Soc., **67** [11] 760–763 (1984).

[17] G.D. Quinn, "Fracture Mechanism Maps for Advanced Structural Ceramics. Part I: Methodology and Hot-Pressed Silicon Nitride Results." MTL TR 90–6, Feb. 1990.

[18] T.-J. Chuang, "A Diffusive Crack-Growth Model for Creep Fracture." J. Am. Ceram. Soc. **65** [2] 93–103 (1982).

REPORT DOCUMENTATION PAGE

Form Approved
OMB No. 0704-0188

1. AGENCY USE ONLY (Leave blank)	2. REPORT DATE	3. REPORT TYPE AND DATES COVERED
	April 1993	Technical Memorandum

4. TITLE AND SUBTITLE

Stress-Rupture Behavior of Small Diameter Polycrystalline Alumina Fibers

5. FUNDING NUMBERS

WU-510-01-50

6. AUTHOR(S)

Hee Mann Yun, Jon C. Goldsby, and James A. DiCarlo

7. PERFORMING ORGANIZATION NAME(S) AND ADDRESS(ES)

National Aeronautics and Space Administration
Lewis Research Center
Cleveland, Ohio 44135-3191

8. PERFORMING ORGANIZATION REPORT NUMBER

E-7979

9. SPONSORING/MONITORING AGENCY NAME(S) AND ADDRESS(ES)

National Aeronautics and Space Administration
Washington, D.C. 20546-0001

10. SPONSORING/MONITORING AGENCY REPORT NUMBER

NASA TM-106256

11. SUPPLEMENTARY NOTES

Prepared for the 95th Annual Meeting and Exposition of the American Ceramic Society, Cincinnati, Ohio, April 18–23, 1993. Hee Mann Yun, Cleveland State University, Cleveland, Ohio 44115 and NASA Resident Research Associate at Lewis Research Center; Jon C. Goldsby, NASA Lewis Research Center; and James A. DiCarlo, NASA Lewis Research Center. Responsible person, Jon C. Goldsby, (216) 433–8250.

12a. DISTRIBUTION/AVAILABILITY STATEMENT

Unclassified - Unlimited
Subject Category 27

12b. DISTRIBUTION CODE

13. ABSTRACT ***(Maximum 200 words)***

Continuous length polycrystalline alumina fibers are candidates as reinforcement in high temperature composite materials. Interest therefore exists in characterizing the thermomechanical behavior of these materials, obtaining possible insights into underlying mechanisms, and understanding fiber performance under long term use. In this paper, results are reported on the time-temperature dependent strength behavior of Nextel 610 and Fiber FP alumina fibers with grain sizes of 100 and 300 nm, respectively. Below 1000 °C and 100 hours, Nextel 610 with the smaller grain size had a greater fast fracture and rupture strength than Fiber FP. The time exponents for stress-rupture of these fibers were found to decrease from ~13 at 900 °C to below 3 near 1050 °C, suggesting a transition from slow crack growth to creep rupture as the controlling fracture mechanism. For both fiber types, an effective activation energy of 690 kJ/mol was measured for rupture. This allowed stress-rupture predictions to be made for extended times at use temperatures below 1000 °C.

14. SUBJECT TERMS

Fibers, Polycrystalline alumina, Stress-rupture; Slow crack growth; Creep rupture

15. NUMBER OF PAGES

14

16. PRICE CODE

A03

17. SECURITY CLASSIFICATION OF REPORT	18. SECURITY CLASSIFICATION OF THIS PAGE	19. SECURITY CLASSIFICATION OF ABSTRACT	20. LIMITATION OF ABSTRACT
Unclassified	Unclassified	Unclassified	